DNA Cage Delivery to Mammalian Cells

Anthony S. Walsh,[†] HaiFang Yin,[‡,§] Christoph M. Erben,[†] Matthew J. A. Wood,[§] and Andrew J. Turberfield[†,*]

[†]Clarendon Laboratory, Department of Physics, University of Oxford, Parks Road, Oxford OX1 3PU, U.K., [‡]Tianjin Research Centre of Basic Medical Science, Tianjin Medical University, Qixiangtai Road, Heping District, Tianjin, 300070, China, and [§]Department of Physiology, Anatomy and Genetics, University of Oxford, South Parks Road, Oxford OX1 3QX, U.K.

ABSTRACT DNA cages are nanometer-scale polyhedral structures formed by self-assembly from synthetic DNA oligonucleotides. Potential applications include *in vivo* imaging and the targeted delivery of macromolecules into living cells. We report an investigation of the ability of a model cage, a DNA tetrahedron, to enter live cultured mammalian cells. Cultured human embryonic kidney cells were treated with a range of fluorescently labeled DNA tetrahedra and subsequently examined using confocal microscopy and flow cytometry. Substantial uptake of tetrahedra into cells was observed both when the cells were treated with tetrahedra alone and when the cells were treated with a mixture of tetrahedra and a transfection reagent. Analysis of the subcellular localization of transfected tetrahedra using confocal microscopy and organelle staining indicates that the cages are located in the cytoplasm. FRET experiments indicate that the DNA cages remain substantially intact within the cells for at least 48 h after transfection. This is a first step toward the use of engineered DNA nanostructures to deliver and control the activity of cargoes within cells.

KEYWORDS: DNA self-assembly · transfection · nanotechnology · nanomedicine · drug delivery

As we become more proficient in the use of information encoded in DNA to direct the assembly[1] and motion[2] of DNA nanostructures, possible applications in biology are beginning to emerge. One of the earliest proposed was the use of DNA scaffolds to create synthetic protein crystals,[3] and recently 2D scaffolds have been used to facilitate protein structure determination by cryo-electron microscopy.[4,5] The ability of nucleic acid systems to compute[6] has suggested the development of autonomous molecular systems for medical diagnosis,[7] and DNA sensors have been used to report intracellular pH[8] and to trigger cell death in response to detection of cancer-inducing mutations.[9] The encapsulation of single molecules of the protein cytochrome *c* within DNA tetrahedra led to the proposal that DNA cages could be used as drug delivery vehicles.[10]

The first DNA cages to be constructed were cubes[11] with edges comprising two turns of the double helix (6.8 nm). The range of polyhedra with double-helical edges has been developed to include another cube,[12] a truncated octahedron,[13] octahedra,[14−16] tetrahedra,[17−20] trigonal bipyramids,[21] dodecahedra,[18] icosahedra,[22,23] and truncated icosahedra[18] as well as hybrid structures with synthetic linkers at vertices[24−26] and larger structures[27−31] based on developments of the DNA origami technique.[32] In addition to proteins,[10] nanoparticles have been encapsulated in DNA polyhedra.[22,25] Folate-modified DNA nanotubes have been shown to be capable of binding to cancer cells overexpressing the folate receptor and of delivering at least some of a covalently attached dye into the cell, although it is not clear whether intact nanotubes are internalized.[33] Preliminary studies have shown that DNA tetrahedra possess an innate resistance to nucleases with a decay time of 42 h in 10% fetal bovine serum.[34]

DNA cages can be designed to change configuration in response to the binding of signal molecules, potentially releasing or allowing access to their cargoes.[24,27,35] If DNA cages were used to transport cargoes into cells, then cage opening, triggered in response to specific biomolecular signals, could be used to control cargo release, creating a smart delivery vehicle with the potential to respond to a particular cell type or state.[35]

Here we show that fluorescently labeled DNA tetrahedra are capable of entering live mammalian cells. Cultured human embryonic kidney (HEK) cells were treated with a range of fluorescently labeled DNA tetrahedra and subsequently examined using confocal microscopy and flow cytometry. Substantial uptake of tetrahedra into cells was observed both when the cells were treated with a mixture of tetrahedra and a transfection reagent and when the cells were treated with tetrahedra alone. Confocal micrographs indicate a punctate distribution within the cytoplasm. Measurement of Förster resonant energy transfer (FRET) between pairs of dyes conjugated to the tetrahedra indicates that they remain substantially intact for at least 48 h after transfection.

RESULTS AND DISCUSSION

DNA tetrahedra were assembled from four 63-nucleotide (nt) oligonucleotides[17]

* Address correspondence to a.turberfield@physics.ox.ac.uk.

Received for review February 11, 2011 and accepted June 22, 2011.

Published online June 22, 2011
10.1021/nn2005574

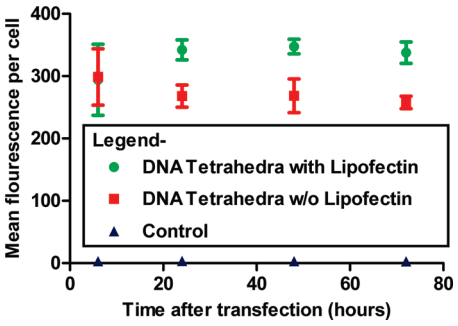

Figure 1. Flow cytometry analysis of the efficiency and stability of transfection with fluorescently labeled DNA cages. The mean fluorescence per cell is similar for cells transfected with and without Lipofectin and is constant for at least 72 h. Control: mock transfection without tetrahedra. Representative cell count histograms are shown in Supporting Figure 3.

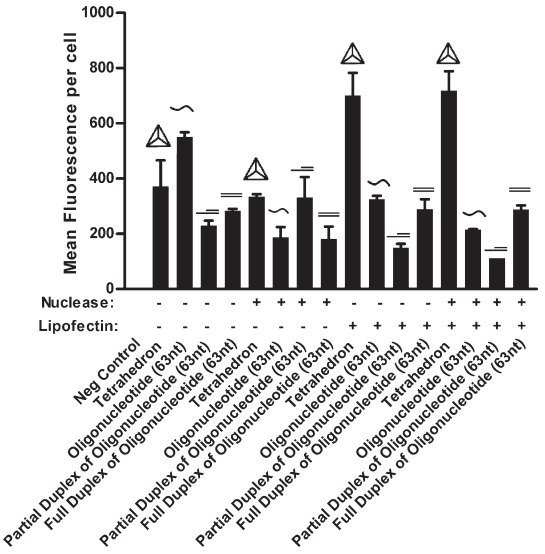

Figure 2. Flow cytometry analysis of transfection efficiencies for a range of fluorescently labeled DNA complexes. Cells were analyzed 24 h post-transfection.

to one of which the dye Cy5 was covalently attached (Supporting Figure 1). Human embryonic kidney cells were plated and incubated with tetrahedra, with and without the addition of the cationic lipid transfection reagent Lipofectin[36] (Invitrogen). Cells were examined by confocal microscopy and flow cytometry at times up to 72 h after transfection. The results of flow cytometry (Figure 1) and confocal microscopy (Supporting Figure 2) are consistent: transfection levels are high both when cells are transfected with naked tetrahedra and when cells are transfected with tetrahedra with the aid of Lipofectin. Levels of fluorescence in transfected cells remain stable for at least 72 h after transfection. (Most cells were confluent at transfection, limiting cell division that would otherwise dilute the fluorescence signal.)

In a complementary test of transfection, biotin-labeled DNA tetrahedra were transfected into cells with and without the aid of Lipofectin. Total DNA was then harvested from transfected cells and dot blotting biotin detection used to assess the levels of intracellular biotin and hence the levels of uptake of the biotin-labeled DNA tetrahedra. The results (Supporting Figure 4) indicate significant levels of biotin in cells transfected with biotin-labeled DNA tetrahedra but not in mock-transfected controls, consistent with the results of fluorescence measurements described above.

Figure 2 shows the results of control experiments designed to compare the efficiencies of transfection with fluorescently labeled DNA tetrahedra and with several other small, fluorescently labeled DNA complexes (Supporting Figure 5): a 63-nt single-stranded oligonucleotide, a partially double-stranded complex of this oligonucleotide, and a fully double-stranded duplex. Transfected cells were analyzed using confocal microscopy (Supporting Figure 6) and flow cytometry (Figure 2) 24 h post-transfection. The highest transfection efficiency recorded was that of the DNA tetrahedron when transfected with the aid of Lipofectin .

A control experiment was carried out to ascertain whether the fluorescence levels measured using flow cytometry represented intracellular fluorescence of transfected complexes or extracellular fluorescence of complexes bound to the outside of the cell membrane. Transfected cells were treated with the promiscuous endonuclease Benzonase (Sigma-Aldrich, UK) before flow cytometry analysis, to digest any complexes bound outside the cells. Nuclease treatment made little difference to fluorescence levels (Figure 2), indicating that the majority of the fluorescence signal corresponds to complexes that have crossed the cell membrane.

Acceptor photobleaching FRET[37] was used to assess the structural integrity of tetrahedra within cells (Figure 3). Two of the component oligonucleotides were fluorescently labeled, with Cy3 and Cy5 (Supporting Figure 1), such that in the doubly labeled tetrahedra the two dyes were approximately 3 nm apart, close enough for significant energy transfer from the photoexcited donor Cy3 to the acceptor Cy5.[38] A mixture of singly labeled tetrahedra, with either the Cy3 or Cy5 modification but not both, was used as a negative control. Regions of high fluorescence (regions of interest, ROI) were identified within confocal sections through transfected cells. Both donor and acceptor fluorescence intensities were recorded before and after intense laser irradiation at the peak of the excitation spectrum of the acceptor, photobleaching acceptor fluorophores within the ROI. Where a donor (Cy3) fluorophore is separated from an acceptor (Cy5) by a distance comparable to the Förster radius (on the order of 6 nm), FRET reduces the intensity of fluorescence from the photoexcited donor: photobleaching of the acceptor, by reducing FRET, therefore increases the intensity of donor fluorescence. In the negative control sample FRET resulting from interactions between rather than within tetrahedra is expected to be weak or negligible. Figure 3 shows frequency distributions of fractional changes

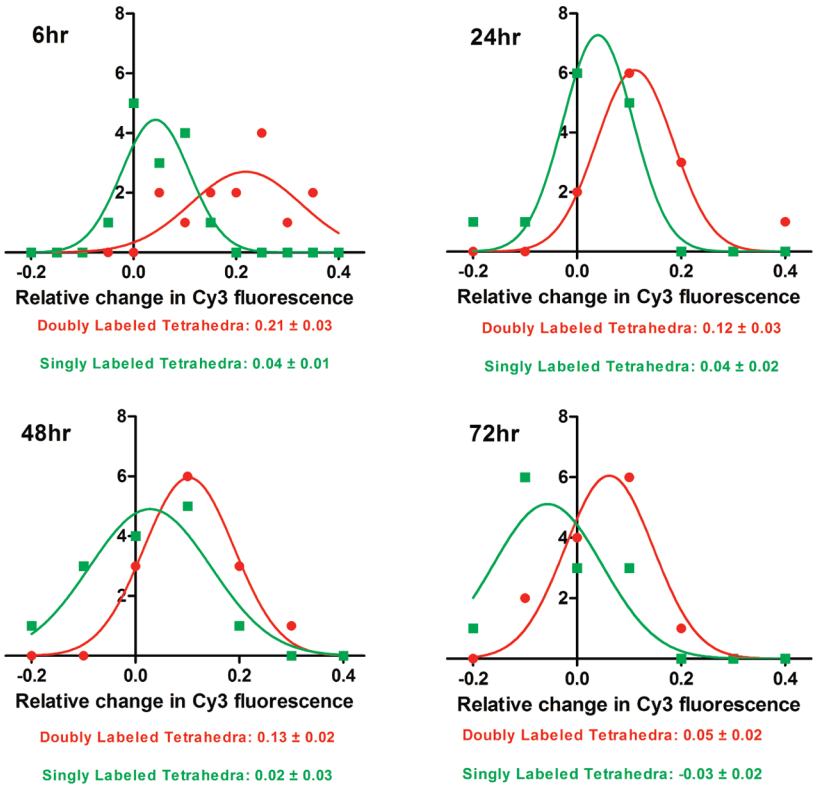

Figure 3. Frequency distributions of relative changes in Cy3 fluorescence following photobleaching of the Cy5 acceptor at different times after transfection: (●) doubly labeled tetrahedra; (■) mixtures of singly labeled (Cy3 or Cy5) tetrahedra (negative control). For each distribution a Gaussian curve with the corresponding mean and standard deviation is plotted, and the mean ± SEM is indicated.

in Cy3 fluorescence, integrated over the ROIs (Supporting Figure 7), after acceptor photobleaching, at times up to 72 h post-transfection. A significant increase in Cy3 fluorescence from cells transfected with doubly labeled tetrahedra indicates that the two dye labels remain bound together within the Förster radius, and thus that the tetrahedra remain substantially intact up to at least 48 h. Very little change in donor fluorescence is observed from the negative control samples.

Confocal micrographs of live HEK cells transfected with Cy5-labeled DNA tetrahedra at a series of times after transfection are shown in Figure 4. Two organelle-specific dyes were used to aid in the determination of intracellular localization: Hoechst 34580 stain (Invitrogen) was used to stain nuclei, and LysoSensor Green (Invitrogen) was used to stain lysosomes. Representative images are shown in Figure 4. Transfected tetrahedra are clearly partitioned to the cytoplasm at all times observed. (Strong nuclear localization of transfected tetrahedra was observed in fixed cells (Supporting Figure 10) but was clearly an artifact of fixation; see Supporting Notes.) The punctate distribution of fluorescence from transfected tetrahedra is similar but not identical to that of the lysosomes, consistent with either aggregation within the cytosol or segregation within organelles that may include lysosomes.

Previous studies have shown that particle size is an important factor in cellular uptake of nanomaterials and that small nanoparticles (with radii <50 nm) exhibit significantly greater uptake than larger particles.[39,40] Spherical nanoparticles have also been shown to be capable of entering cells more effectively than cylindrical or filamentous nanoparticles.[41] DNA tetrahedra are small (maximum dimension ~7 nm) and relatively compact, so these findings are consistent with the effective cellular uptake of DNA tetrahedra reported here. There are several possible routes for entry of nanoparticles into cells, including macropinocytosis, clathrin-mediated endocytosis, and caveolae-mediated endocytosis.[42] Further investigation will be required to determine the exact mechanism or mechanisms by which DNA cages enter cells.

In order to assess the intracellular localization of transfected DNA tetrahedra in relation to the microtubule-organizing centers, live HEK cells were co-transfected with a centrin-GFP expression plasmid[43] and with Cy5-labeled DNA tetrahedra. The fluorescent centrin-GFP fusion indicates the positions of the microtubule-organizing centers. Figure 5 contains confocal micrographs recorded at a series of times after transfection: There is a gradual movement of transfected cages from a punctate to a more diffuse pattern of distribution throughout the cytoplasm with some indication

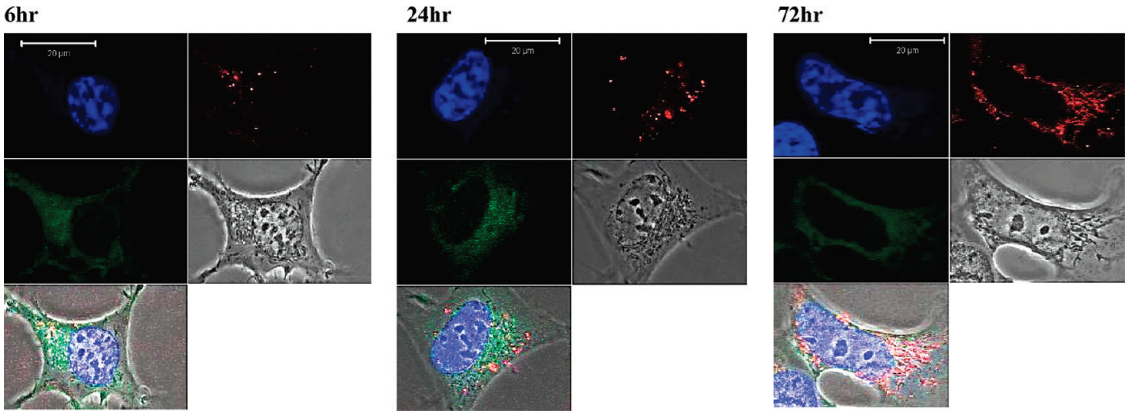

Figure 4. Confocal micrographs of HEK cells showing intracellular localization of Cy5-labeled DNA tetrahedra transfected without the aid of a transfection reagent. Images of nuclear and lysosome organelle stains are shown for reference. Time after transfection is shown in hours. Blue: nuclear stain; red: Cy5; green: LysoSensor (lysosomes); gray: phase contrast. Scale bars: 20 μm. Two additional time points (48 and 60 h) are shown in Supporting Figure 8.

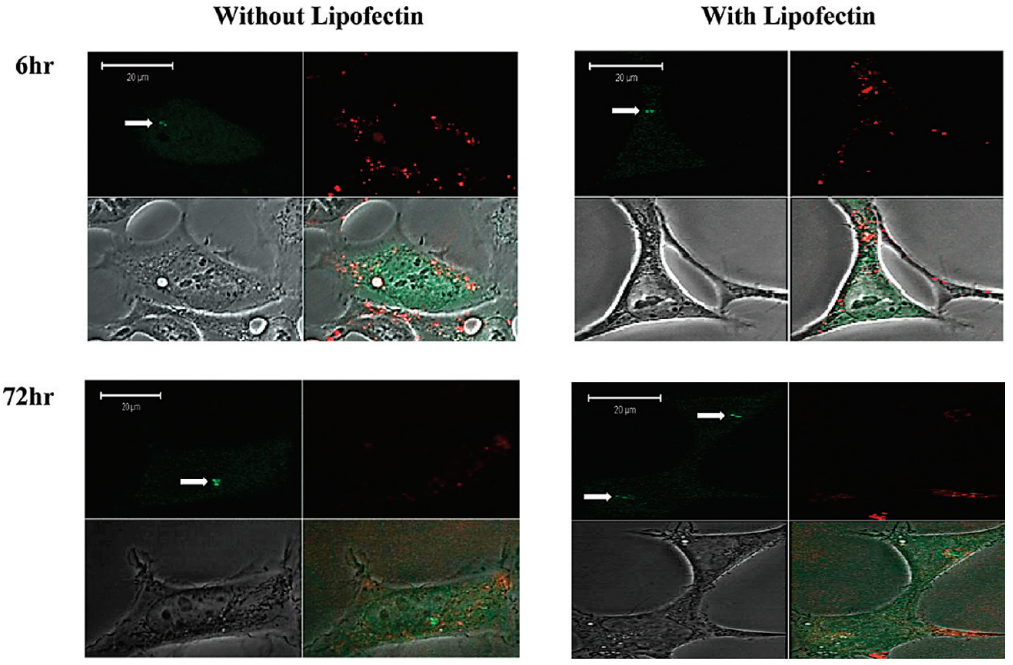

Figure 5. Intracellular localization of transfected Cy5-labeled tetrahedra. Images of centrin-GFP fluorescence are shown for reference. Time after transfection is shown in hours. Green: centrin-GFP; red: Cy5; gray: phase contrast. White arrows indicate the locations of pairs of microtubule-organizing centers. Scale bar: 20 μm. Three additional time points (24, 48, and 60 h) are shown in Supporting Figure 9.

of localization around the microtubule-organizing centers. Further work is required in order to determine whether or not the transfected tetrahedra are following a microtubule-mediated endocytic pathway.[44]

In summary, we have shown that DNA tetrahedra can enter cultured mammalian cells and that they do so effectively both with and without the aid of a transfection reagent. Transfected tetrahedra remain substantially intact and are localized within the cytoplasm; the transfection mechanism and the degree of access of transfected tetrahedra to the cytosol require further study. These results represent an important first step as proof of concept in efforts to use DNA cages to deliver cargoes and to control their activities within cells.

MATERIALS AND METHODS

Preparation of DNA Tetrahedra. DNA tetrahedra were synthesized and purified following the methods described in ref 17. Component oligonucleotides were purchased from Integrated DNA Technologies (USA). Nucleotide sequences and schematic diagrams of the tetrahedra are shown in Supporting Figure 1.

Transfection of Cells. One day before transfection, samples of HEK cells were plated in glass-bottomed 35 mm Petri dishes in

growth medium (Dulbecco's modified Eagle's medium (Gibco, USA)) containing 10% fetal bovine serum, 1% glutamine, and 1% penicillin and streptomycin. Cells (3×10^5) were seeded in each dish (as estimated using a hemocytometer). Cells were incubated overnight at 37 °C in a humidified atmosphere containing 5% CO_2.

Lipofectin (Invitrogen, USA) was diluted 50-fold (to a final volume of 100 μL) in Opti-MEM (serum-free medium) (Gibco, USA) and left at room temperature for 45 min. A sample containing 1 μg of DNA tetrahedra was diluted to 100 μL with Opti-MEM, combined with the diluted Lipofectin mixture, and left for 20 min at room temperature. The mixture was then made up to 1.5 mL with Opti-Mem.

Growth medium was removed from each cell sample, and the cells were washed twice with phosphate-buffered saline (PBS) (Gibco, USA). Each transfection mixture was then added to a sample of cells and incubated for 3–4 h at 37 °C in a humidified atmosphere containing 5% CO_2. Cells were then washed three times with PBS. Growth medium (2 mL) was added to each dish, and the transfected cells were stored in an incubator at 37 °C in a humidified atmosphere containing 5% CO_2 until it was time for them to be examined.

Transfection of DNA tetrahedra without the aid of Lipofectin was performed as described above, using 1 μg samples of tetrahedra diluted to 1.5 mL with Opti-MEM.

Confocal Microscopy. Immediately before examination, growth medium was removed from the wells and the cells were washed with PBS three times. Fresh growth medium was then added. Live cells were imaged using a LSM 510 META inverted fluorescence confocal microscope (Carl Zeiss International).

Filters used were 543 nm Ex/560–615 nm for Cy3, 633 nm Ex/657–679 nm for Cy5, 458 nm Ex 486–518 nm for Lysosensor Green, and 405 nm Ex/422–465 nm for Hoechst 34580.

The microscope laser (HeNe Laser, 633 nm, 5 mW) was used to bleach Cy5 in selected areas of transfected cells (ROIs) by repeated scanning. An example of an ROI is shown in Supporting Figure 6. Cy3 fluorescence was recorded both before and after bleaching and integrated over the ROI. At least 13 regions were examined for each experimental condition.

Subcellular organelles were stained in order to assess the subcellular localization of transfected tetrahedra. LysoSensor Green (DND-189, Invitrogen, USA) was added to the growth medium of the cells to be stained to a final concentration of 1 μM. After incubation for 15 min at 37 °C in a humidified 5% CO_2 atmosphere, Hoechst stain (Hoechst 34580, Invitrogen USA) was added to the growth medium to a final concentration of 0.5 μg/mL. Cells were incubated for a further 15 min before being washed and examined.

Microtubule-organizing centers were labeled by transfecting cells with the pEGFP-CETN2 plasmid.[43] Transfection of the plasmid was carried out with the aid of the transfection reagent Lipofectamine 2000 (Invitrogen, USA) following the manufacturer's instructions. A 1 μg sample of plasmid was added to each dish of cells before transfection with tetrahedra as described above.

Flow Cytometry. Results shown in Figures 1 and 2 were obtained using the following flow cytometry methods. Growth medium was removed and cells were washed with PBS. Then 0.6 mL of trypsin replacement (TrypLE express stable trypsin replacement enzyme without phenol red, Gibco, USA) was added to each sample, and the samples were incubated for 5 min at 37 °C. Then 1 mL of PBS was added to each sample, and the resulting cell suspensions were transferred to Falcon tubes and centrifuged for 3 min at 2500 rpm. Supernatant was removed, and the cell pellets were resuspended in 1 mL of PBS. The cells were then centrifuged and resuspended in fresh PBS. Samples of at least 1000 cells were analyzed in duplicate and triplicate using a FACS Calibur flow cytometer (BD Biosciences, USA). Consistent gating based on cell size and granularity (forward and side scatter) was applied to select only fluorescence measurements from healthy cells.

Benzonase nuclease treatment prior to flow cytometry analysis was carried out by incubating the cells for 10 min with a solution of PBS containing at least 500 U/mL of the nuclease prior to trypsinization. The cells were then washed with PBS before being prepared for flow cytometry analysis as described above.

Supporting Notes. In initial experiments, transfected cells were prepared for confocal microscopy by methanol fixation. Representative micrographs are shown in Supporting Figure 10. Strong Cy3 and Cy5 signals, co-localized with the nuclear stain DAPI, indicated efficient localization of the tetrahedra to the nucleus. However, micrographs of live, unfixed transfected cells show cytoplasmic localization (Figure 4, Supporting Figures 6, 8, and 9), suggesting that the nuclear localization observed with methanol fixation was an artifact. Observation of nuclear localization of a viral protein (herpes simplex VP22) has been shown to be an artifact of methanol fixation.[45]

Supporting Information Available: DNA tetrahedra used in transfection experiments; time courses of intracellular distributions of tetrahedra transfected with and without Lipofectin; representative cell count histograms for data shown in Figure 1; detection of transfection by biotin-labeled tetrahedra; DNA complexes used in control transfection experiments; comparison between intracellular distributions of fluorescently labeled DNA complexes used for transfection; confocal micrographs showing the photobleaching of an ROI; additional time points for Figures 4, 5; representative confocal micrographs of fixed cells transfected with fluorescently labeled DNA tetrahedra. This information is available free of charge *via* the Internet at http://pubs.acs.org.

REFERENCES AND NOTES

1. Seeman, N. C. DNA in a Material World. *Nature* **2003**, *421*, 427–431.
2. Bath, J.; Turberfield, A. J. DNA Nanomachines. *Nat. Nanotechnol.* **2007**, *2*, 275–84.
3. Seeman, N. C. Nucleic-acid Junctions and Lattices. *J. Theor. Biol.* **1982**, *99*, 237–247.
4. Malo, J.; Mitchell, J. C.; Vénien-Bryan, C.; Harris, J. R.; Wille, H.; Sherratt, D. J.; Turberfield, A. J. Engineering a 2D Protein-DNA Crystal. *Angew. Chem., Int. Ed.* **2005**, *44*, 3057–3061.
5. Selmi, D. N.; Adamson, R. J.; Attrill, H.; Goddard, A.; Gilbert, R. J. C.; Watts, A.; Turberfield, A. J. DNA-Templated Protein Arrays for Single-Molecule Imaging. *Nano Lett.* **2011**, *11*, 657–660.
6. Adleman, L. Molecular Computation of Solutions to Combinatorial Problems. *Science* **1994**, *266*, 1021–1024.
7. Benenson, Y.; Gil, B.; Ben-Dor, U.; Adar, R.; Shapiro, E. An Autonomous Molecular Computer for Logical Control of Gene Expression. *Nature* **2004**, *429*, 423–429.
8. Modi, S.; Swetha, M. G.; Goswami, D.; Gupta, G. D.; Mayor, S.; Krishnan, Y. A DNA Nanomachine that Maps Spatial and Temporal pH Changes Inside Living Cells. *Nat. Nanotechnol.* **2009**, *4*, 325–330.
9. Venkataraman, S.; Dirks, R. M.; Ueda, C. T.; Pierce, N. A. Selective Cell Death Mediated by Small Conditional RNAs. *Proc. Natl. Acad. Sci. U. S. A.* **2010**, *107*, 16777–16782.
10. Erben, C. M.; Goodman, R. P.; Turberfield, A. J. Single-Molecule Protein Encapsulation in a Rigid DNA Cage. *Angew. Chem., Int. Ed.* **2006**, *45*, 7414–7417.
11. Chen, J. H.; Seeman, N. C. Synthesis from DNA of a Molecule with the Connectivity of a Cube. *Nature* **1991**, *350*, 631–633.
12. Zhang, C.; Ko, S. H.; Su, M.; Leng, Y.; Ribbe, A. E.; Jiang, W.; Mao, C. Symmetry Controls the Face Geometry of DNA Polyhedra. *J. Am. Chem. Soc.* **2009**, *131*, 1413–1415.
13. Zhang, Y.; Seeman, N. C. Construction of a DNA-Truncated Octahedron. *J. Am. Chem. Soc.* **1994**, *116*, 1661–1669.
14. Shih, W. M.; Quispe, J. D.; Joyce, G. F. A 1.7-kilobase Single-Stranded DNA that Folds into a Nanoscale Octahedron. *Nature* **2004**, *427*, 618–621.
15. He, Y.; Su, M.; Fang, P. A.; Zhang, C.; Ribbe, A. E.; Jiang, W.; Mao, C. On the Chirality of Self-Assembled DNA Octahedra. *Angew. Chem., Int. Ed.* **2010**, *49*, 748–751.
16. Andersen, F. F.; Knudsen, B.; Oliveira, C. L. P.; Frohlich, R. F.; Kruger, D.; Bungert, J.; Agbandje-McKenna, M.; McKenna, R.; Juul, S.; Veigaard, C.; *et al.* Assembly and Structural

Analysis of a Covalently Closed Nano-Scale DNA Cage. *Nucleic Acids Res.* **2008**, *36*, 1113–1119.
17. Goodman, R. P.; Schaap, I. A.; Tardin, C. F.; Erben, C. M.; Berry, R. M.; Schmidt, C. F.; Turberfield, A. J. Rapid Chiral Assembly of Rigid DNA Building Blocks for Molecular Nanofabrication. *Science* **2005**, *310*, 1661–1665.
18. He, Y.; Ye, T.; Su, M.; Zhang, C.; Ribbe, A. E.; Jiang, W.; Mao, C. Hierarchical Self-Assembly of DNA into Symmetric Supramolecular Polyhedra. *Nature* **2008**, *452*, 198–201.
19. Li, Z.; Wei, B.; Nangreave, J.; Lin, C.; Liu, Y.; Mi, Y.; Yan, H. A Replicable Tetrahedral Nanostructure Self-Assembled from a Single DNA Strand. *J. Am. Chem. Soc.* **2009**, *131*, 13093–13098.
20. Kato, T.; Goodman, R. P.; Erben, C. M.; Turberfield, A. J.; Namba, K. High-Resolution Structural Analysis of a DNA Nanostructure by CryoEM. *Nano Lett.* **2009**, *9*, 2747–2750.
21. Erben, C. M.; Goodman, R. P.; Turberfield, A. J. A Self-Assembled DNA Bipyramid. *J. Am. Chem. Soc.* **2007**, *129*, 6992–6993.
22. Bhatia, D.; Mehtab, S.; Krishnan, R.; Indi, S. S.; Basu, A.; Krishnan, Y. Icosahedral DNA Nanocapsules by Modular Assembly. *Angew. Chem., Int. Ed.* **2009**, *48*, 4134–4137.
23. Zhang, C.; Su, M.; He, Y.; Zhao, X.; Fang, P. A.; Ribbe, A. E.; Jiang, W.; Mao, C. Conformational Flexibility Facilitates Self-Assembly of Complex DNA Nanostructures. *Proc. Natl. Acad. Sci. U. S. A.* **2008**, *105*, 10665–10669.
24. Aldaye, F. A.; Sleiman, H. F. Modular Access to Structurally Switchable 3D Discrete DNA Assemblies. *J. Am. Chem. Soc.* **2007**, *129*, 13376–13377.
25. Yang, H.; McLaughlin, C. K.; Aldaye, F. A.; Hamblin, G. D.; Rys, A. Z.; Rouiller, I. R.; Sleiman, H. F. Metal-Nucleic Acid Aages. *Nat. Chem.* **2009**, *1*, 390–396.
26. Zimmermann, J.; Cebulla, M. P.; Monninghoff, S.; von Kiedrowski, G. Self-Assembly of a DNA Dodecahedron from 20 Trisoligonucleotides with C-3h Linkers. *Angew. Chem., Int. Ed.* **2008**, *47*, 3626–3630.
27. Andersen, E. S.; Dong, M.; Nielsen, M. M.; Jahn, K.; Subramani, R.; Mamdouh, W.; Golas, M. M.; Sander, B.; Stark, H.; Oliveira, C. L. P.; *et al.* Self-Assembly of a Nanoscale DNA Box with a Controllable Lid. *Nature* **2009**, *459*, 73–75.
28. Dietz, H.; Douglas, S. M.; Shih, W. M. Folding DNA into Twisted and Curved Nanoscale Shapes. *Science* **2009**, *325*, 725–730.
29. Douglas, S. M.; Dietz, H.; Liedl, T.; Högberg, B.; Graf, F.; Shih, W. M. Self-Assembly of DNA into Nanoscale Three-Dimensional Shapes. *Nature* **2009**, *459*, 414–418.
30. Endo, M.; Hidaka, K.; Kato, T.; Namba, K.; Sugiyama, H. DNA Prism Structures Constructed by Folding of Multiple Rectangular Arms. *J. Am. Chem. Soc.* **2009**, *131*, 15570–15571.
31. Ke, Y.; Sharma, J.; Liu, M.; Jahn, K.; Liu, Y.; Yan, H. Scaffolded DNA Origami of a DNA Tetrahedron Molecular Container. *Nano Lett.* **2009**, *9*, 2445–2447.
32. Rothemund, P. W. Folding DNA to Create Nanoscale Shapes and Patterns. *Nature* **2006**, *440*, 297–302.
33. Ko, S.; Liu, H.; Chen, Y.; Mao, C. DNA Nanotubes as Combinatorial Vehicles for Cellular Delivery. *Biomacromolecules* **2008**, *9*, 3039–3043.
34. Keum, J. W.; Bermudez, H. Enhanced Resistance of DNA Nanostructures to Enzymatic Digestion. *Chem. Commun. (Cambridge, U. K.)* **2009**, *45*, 7036–7038.
35. Goodman, R. P.; Heilemann, M.; Doose, S.; Erben, C. M.; Kapanidis, A. N.; Turberfield, A. J. Reconfigurable, Braced, Three-Dimensional DNA Nanostructures. *Nat Nanotechnol.* **2008**, *3*, 93–96.
36. Felgner, P. L.; Gadek, T. R.; Holm, M.; Roman, R.; Chan, H. W.; Wenz, M.; Northrop, J. P.; Ringold, G. M.; Danielsen, M. Lipofection: a Highly Efficient, Lipid-Mediated DNA-Transfection Procedure. *Proc. Natl. Acad. Sci. U. S. A.* **1987**, *84*, 7413–7417.
37. Kenworthy, A. K. Imaging Protein-Protein Interactions using Fluorescence Resonance Energy Transfer Microscopy. *Methods* **2001**, *24*, 289–296.
38. Stryer, L.; Haugland, R. P. Energy Transfer: a Spectroscopic Ruler. *Proc. Natl. Acad. Sci. U. S. A.* **1967**, *58*, 719–726.
39. Gao, H.; Shi, W.; Freund, L. B. Mechanics of Receptor-Mediated Endocytosis. *Proc. Natl. Acad. Sci. U. S. A.* **2005**, *102*, 9469–9474.
40. Prabha, S.; Zhou, W. Z.; Panyam, J.; Labhasetwar, V. Size-Dependency of Nanoparticle-Mediated Gene Transfection: Studies with Fractionated Nanoparticles. *Int. J. Pharm.* **2002**, *244*, 105–115.
41. Geng, Y.; Dalhaimer, P.; Cai, S.; Tsai, R.; Tewari, M.; Minko, T.; Discher, D. E. Shape Effects of Filaments versus Spherical Particles in Flow and Drug Delivery. *Nat. Nanotechnol.* **2007**, *2*, 249–255.
42. Hillaireau, H.; Couvreur, P. Nanocarriers' Entry into the Cell: Relevance to Drug Delivery. *Cell. Mol. Life Sci.* **2009**, *66*, 2873–2896.
43. White, R. A.; Pan, Z.; Salisbury, J. L. GFP-Centrin as a Marker for Centriole Dynamics in Living Cells. *Microsc. Res. Tech.* **2000**, *49*, 451–457.
44. Hasegawa, S.; Hirashima, N.; Nakanishi, M. Microtubule Involvement in the Intracellular Dynamics for Gene Transfection Mediated by Cationic Liposomes. *Gene Ther.* **2001**, *8*, 1669–1673.
45. Lundberg, M.; Johansson, M. Is VP22 Nuclear Homing an Artifact? *Nat. Biotechnol.* **2001**, *19*, 713–714.